J|A|C|S COMMUNICATIONS

Published on Web 05/11/2010

Nanocomposites with Spatially Separated Functionalities for Combined Imaging and Magnetolytic Therapy

Shang-Hsiu Hu[†,‡] and Xiaohu Gao*[,†]

Department of Bioengineering, University of Washington, William H. Foege Building N530M, Seattle, Washington 98195, and Department of Materials Sciences and Engineering, National Chiao Tung University, Hsinchu, Taiwan

Received March 25, 2010; E-mail: xgao@u.washington.edu

Compact nanostructures with highly integrated functionalities are of considerable current interest to research fields such as drug delivery, multimodality imaging, and electronic devices.[1] A key challenge, however, is how to combine individual components together without interfering or sacrificing their original electronic and optical properties.[2] On the nanometer scale, fascinating work by Xu, Teranishi, and Banin has produced a variety of heterodimer structures composed of quantum dots, magnetic nanoparticles (MNPs), and metallic NPs. Because the different components are touching each other, their signature optical, magnetic, and electronic properties are often altered[3d] or completely lost.[3f] In addition, despite the excellent similarity and compatibility in size between these heterodimer nanocrystals and biomolecules, often their small sizes also limit their response to external stimuli. For example, the magnetic domains (few nanometers) in these heterodimers do not respond to external magnetic fields efficiently (particles move slowly in magnetic fields). In parallel, the functionality interferences between different building blocks are also commonly observed on the micrometer scale. For example, doping fluorophores with MNPs in microspheres leads to significant fluorescence quenching.

A simple solution to this interference problem is to engineer multifunctional particles with individual building blocks spatially separated. Toward this end, microspheres with asymmetric architectures, also known as Janus particles, have been produced routinely. They offer unique features, such as precisely controlled distribution of surface charges, compositions, hydrophobicity and hydrophilicity, dipole moments, combined and modular functionalities, which enable important applications unavailable to their symmetrical counterparts. For example, Kopelman and co-workers reported the preparation of modulated optical nanoprobes (MOONs) based on submicrometer fluorescent spheres with one side capped with metal shells, which block light transmittance.[4] Due to size-dependent rotational Brownian motion, the signature frequency of fluorescence fluctuation provides a unique mechanism for identification of the MOONs. Similarly, in device engineering, asymmetric structure also allows remote control of particle movement by electrical and magnetic fields, a promising strategy for engineering electronic paper, displays,[5] and potentially spintronic memory devices.[6] Creative applications unique to asymmetric particles also include catalysis. Crossley et al. recently developed NPs located at the interface of aqueous and organic solvents, which opens new opportunities for multistep reactions that occurs in different solvents.[7]

Despite these recent excitements and the strong need of multifunctionalities, asymmetric particles have found limited applications in biomedical research, to a significant degree, due to the size mismatch between the current Janus microspheres and the biological systems. On the length scale of micrometers, synthetic approaches based on microfluidics, phase separation, and toposelective surface modification for making uniform Janus colloids of tunable composition are well-established. However, a key problem is that the sizes of these colloids range from one to hundreds of micrometers,[8] which are too big for bioapplications such as molecular imaging, drug delivery, and biomolecule labeling. Therefore, there is a strong need for technologies that can make compact nanocomposites with spatially separated functionalities, uniform size, tunable composition, and efficient response to stimuli for applications in biological research.

To address this technical challenge, here, we report a simple, versatile, and scalable synthetic approach based on microemulsion, free of small-molecule surfactants, and controlled phase separation. A magneto-optical combination by incorporating fluorophores and MNPs in separate compartments is used to demonstrate the concept. The resulting nanocomposites share virtually all the desirable properties with the conventional Janus microspheres while simultaneously being compact in size. We further demonstrate magnetic field modulated imaging and an innovative application of this technology in cancer cell therapeutics based on magnetically controlled mechanical forces, which we name magnetolytic therapy.

To incorporate the functionality of responsiveness to environmental stimuli, MNPs are used as one of the building blocks for remote modulation with magnetic fields. As shown in Figure 1a, hydrophobic MNPs (5 nm) and an amphiphilic block copolymer, poly(styrene-block-allyl alcohol) (PS_{16}-*b*-PAA_{10}, M.W. 2200), are mixed in an organic solvent (chloroform) at various ratios, whereas polyvinyl alcohol (PVA, M.W. 9000) is dissolved in water. A fluorescent dye, pyrene, is used to label the polymer phase for optical detection. We select PVA over common small-molecule surfactants because of not only its emulsifying capability but also more importantly its outstanding biocompatibility, which is important for applications oriented toward biology and medicine. Note that due to the broad availability of NPs, polymers, and fluorophores, the composition of the resulting biphasic nanocomposites is highly flexible. The combination of MNPs and pyrene labeled PS-*b*-PAA merely represents a proof-of-concept. Ultrasonic emulsification is used to emulsify the solution mixture, followed by slow evaporation of the organic phase, leading to formation of compact and uniform nanocomposites.

Figure 1b shows the transmission electron microscopy (TEM) images of the nanocomposites. The particles are well dispersed and uniform with an average diameter of approximately 180 nm. Some small particles are also observed under TEM, which can be readily removed by size-selective centrifugation. Regardless of the size, the volume ratios of the embedded MNPs and polymers appear to be identical. This is perhaps not too surprising since the ratio is determined by the initial concentrations of MNPs and polymers in the organic phase. During emulsification, the amounts of MNPs

[†] University of Washington.
[‡] National Chiao Tung University.

10.1021/ja102489q

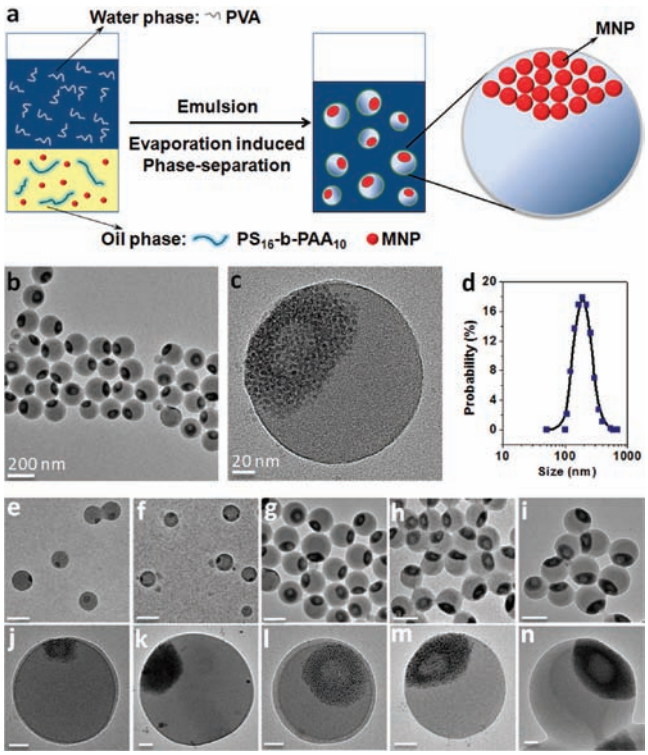

Figure 1. (a) Schematic illustration of the key steps involved in the synthesis of multifunctional nanocomposites with spatially separated functionalities. (b and c) TEM of the magneto-optical nanocomposites at magnifications of 10 K and 60 K. (d) Hydrodynamic size (190 ± 38 nm) of the nanocomposites in aqueous solution. (e−n) Composition tunability of the magneto-optical biphasic particles studied with TEM. Increasing concentrations of MNPs increase the size of the nanocomposites and their magnetic segments. Scale bars: (e−i) 200 nm and (j−n) 20 nm.

and polymers distribute into small droplets proportional to the droplet size. TEM images of higher magnification (Figure 1c) clearly reveal the biphasic structure with MNPs assembled on one side and polymers on the other, resulting from evaporation-induced phase separation between the two building blocks. Note that the MNPs used in the current study are superparamagnetic and do not aggregate spontaneously before solvent evaporation. When their concentration reaches saturation value, they agglomerate driven by van der Waals interaction. Under current experimental conditions, MNPs precipitate out first as the organic phase slowly dries because their solubility is significantly lower than that of the polymers (Figure S1). Similar behavior has been observed previously in immiscible polymer blends and large microspheres as well.[8h,9] The composites phase separate into a Janus structure rather than core−shell structure, likely resulting from minimization of interfacial tensions.

The uniformity of the resulting biphasic nanocomposites is also confirmed by dynamic light scattering (DLS) measurements. Figure 1d displays a hydrodynamic diameter of 190 nm for the same batch of particles, confirming excellent colloidal dispersity in aqueous solution without the need of other surfactants, stabilizers, or chemical modifications to the surface. The importance of microemulsion methods in making biphasic NPs has also been realized by other researchers. For example, Isojima et al. recently reported polymer nanoparticles with MNPs coated on one side.[10] Unfortunately, the resulting particles are not uniform and the MNPs are only attached to the bead surface, which could result in separation with the polymer particles. It is noteworthy that although microemulsions typically generate polydisperse particles, our current emulsion system produces relatively uniform NPs. Furthermore, in contrast to the microfluidics method (makes beads one at a time) and the toposelective surface modification (makes a small number depending on surface area) commonly used in engineering micrometer-sized Janus particles, this wet-chemistry-based technology offers similar capabilities but is highly scalable in production.

To probe the composition tunability of this technology, which is another common feature for Janus microspheres but difficult to achieve for NPs, we varied the quantity of MNPs in the initial stock solutions while keeping the polymer concentration constant. TEM images in Figure 1e−n clearly reveal that the increasing concentrations of MNPs not only produce larger MNP phases in the composites but also increase the overall particle sizes. As the weight ratio of MNP/polymer increases from 3.7 to 60%, the size of the composite particles increases from ∼120 to 220 nm (Table S1). Despite the apparent correlation between the initial MNP concentration in chloroform and the final MNP volume inside the nanocomposites, we are not able to determine the exact volume ratios between the MNP and polymer segments. This is due to the irregular shapes of the two segments and the difficulty in visualizing all three dimensions of the MNP segments from TEM images (2-D projections). In contrast, for Janus microspheres with flat cross sections (two truncated spheres), well-established models have been developed to calculate the volume ratio of the two phases.[8f] In addition, it is also interesting to observe a shallow dimple site in the MNP segment. Previous studies by Saito et al. has shown that when PVA is used as the stabilizer for emulsion of polymer/toluene solutions in water, the surface of the solidified particles always has a dimple due to evaporation of a small amount of organic solvent initially trapped inside the beads.[11]

Using the new multifunctional nanocomposites, we investigated their responses to external stimuli, which will serve as the basis for potential applications in medicine and electronics. For example, responses to spinning magnetic fields and the resulting mechanical forces could become an effective approach for cancer treatment and solve the size problem (too big) encountered by magnetic-vortex microdiscs.[12] Similarly, a quick response to magnetic fields is also desirable to fabricate smart displays.[5,13] To magnetically modulate the orientation, the magneto-optical nanocomposites were placed between two glass coverslips for optical imaging and microscopy. As schematically illustrated in Figure 2a, a magnet was first placed immediately below the sample to make the MNP phase face down. When placed onto the stage of an inverted microscope where both incident light and fluorescence travel through objectives on the bottom, fluorescence should be significantly reduced due to blockage of the excitation and emission. Next,

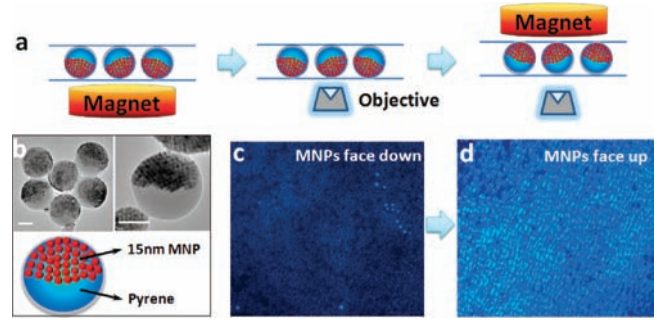

Figure 2. Orientation dependent fluorescence of magneto-optical biphasic nanocomposites. (a) Schematic of nanocomposite orientation modulation with magnetic fields. The magnetic segment blocks both excitation and fluorescence when it is facing down but has no effect on fluorescence when facing up (not in the light path). (b) TEM images of the nanocomposites with the two phases of similar volume. Scale bar 100 nm. (c and d) Fluorescence imaging of nanocomposites of opposite orientations.

when the magnet is placed on top of the coverslips to switch the orientation of the magneto-optical biphasic nanocomposites, fluorescence should be expected because neither excitation nor emission is blocked. For efficient light blocking, we prepared nanocomposites with two phases of approximately the same volume (hemispheres, Figure 2b).

Figure 2c,d shows a remarkable difference in fluorescence intensity with or without MNP blocking. The quenching effect is likely dominated by attenuation of both excitation light (350 ± 20 nm) and emitted fluorescence (>420 nm) in the light path since MNPs are stronger absorbers in the UV and visible spectra. For a small amount of pyrene molecules partitioned into the MNP phase or located at the boundary of the two phases, additional quenching effects such as energy transfer through dipole coupling are also possible. Regardless of the quenching mechanisms, the imaging results clearly demonstrated the responsiveness of the biphasic nanocomposites to external magnetic fields and tunable fluorescence depending on the directions of incident and emitted lights. This magnetic field modulated fluorescence is unique to the nanocomposites with spatially separated functionalities. In contrast, composites with fluorophores and MNPs mixed homogeneously should remain in the low fluorescence state at all times. It is also noteworthy that, despite the efficient response to magnetic fields, the nanocomposites do not agglomerate in solution in the absence of magnetic fields, which is essential for biomedical uses. They remain independent in solution because the magnetic compartment is not composed of a large ferromagnet but an ensemble of small superparamagnetic NPs whose magnetic moments average to zero collectively.

We further demonstrated an innovative application of this technology, magnetolytic therapy, which is achieved through magnetic field modulated cell membrane damage. As schematically illustrated in Figure 3a, the nanocomposites can be quickly attached to the cell surface using a magnetic field for both imaging and treatment. Indeed, fluorescence imaging confirms that the nanocomposites can coat the cell surface at high density within 3 min (Figure 3b). In the current communication, the cell−particle attachment is achieved through nonspecific adsorption facilitated by magnetic manipulation, and we speculate that specific targeting of a certain type of cells by linking the nanocomposites with targeting ligands should also be possible.[1b,14] To probe the therapeutic effect of the particles, cells were placed in a spinning magnetic field (50 rpm), which creates a mechanical force on the cell membrane. Previous research by Kim et al. using magnetic microdisks and a similar low frequency field achieved ~90% cancer-cell destruction *in vitro*.[12] The therapeutic effect came from two mechanisms, the compromised integrity of the cell membrane and promoted apoptosis, in contrast to the more common magneto-thermal effect, which requires a high-frequency oscillating magnetic field. The micrometer sized disks could encounter problems *in vivo* such as blockage of capillary vessels and limited tumor penetration depth. The more compact nanocomposites could help solve this problem. Figure 3f shows that after 15-min exposure to the spinning magnetic field, the majority of the tumor cells were killed, identified by Trypan blue staining. In contrast, control experiments, where either the nanocomposites or the magnetic fields are missing, show virtually no effect on cell viability. This magnetic induction specificity could provide important advantages for image-guided *in vivo* therapy, because NP-based therapeutics regardless of surface coating (nonfouling polymers such as polyethylene glycol or dextran) and targeting ligands (e.g., antibody and peptide) always show some degree of nonspecific uptake by the reticulo-endothelial systems. Image guided local magnetic field induction at the diseased sites could help reduce therapeutic side effects.

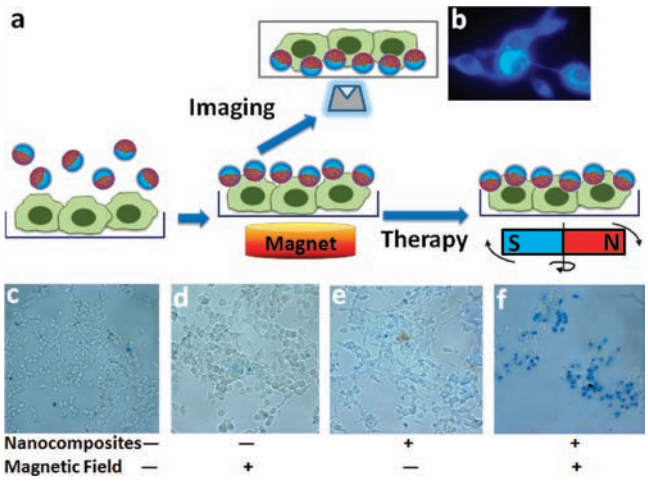

Figure 3. Simultaneous imaging and treatment of cancer cells using biphasic nanocomposites. (a) Schematic illustration of the experimental conditions and magnetolytic therapy. Nanocomposites are first brought down to cell surface by magnetic attraction. Cells can then be examined by fluorescence microscopy or treated with oscillating magnetic fields, which result in mechanical forces to break down cell membranes. (b) Fluorescence imaging of cells coated with nanocomposites. (c−f) Magnetolytic therapy on tumor cells. In comparison with the controls, missing either magnetic fields or nanocomposites, the viability of cells exposed to both is significantly reduced (dead cells appear blue due to Trypan blue staining). Note the low cell density in the treatment group (f) resulting from detachment of dead cells from cell culture dishes. The number of live cells in (f) compared with that in (c) is reduced by 77%, whereas those in (d) and (e) show greater than 99.5% cell survival.

In summary, we have developed a new technology for making composite NPs with spatially separated functionalities. These particles are simultaneously multifunctional, compact in size, and sensitive to environmental stimulation, features which are not available for conventional Janus microspheres and inorganic dumbbell nanocrystals. Due to the broad availability of nanoparticular and molecular building blocks, the compositions of the multifunctional biphasic NPs are highly modular depending on desired applications. Toward biomedical applications, we have demonstrated orientation control of the nanocomposites by external magnetic fields, cell imaging, and an innovative magnetolytic therapy on tumor cells. Future development of this new class of multifunctional nanocomposites includes targeted imaging and therapy *in vitro* and *in vivo*, and we envision this enabling technology will open exciting opportunities in nanomedicine, electronics, spintronics, and catalysis.

Acknowledgment. This work was supported in part by grants to X.H.G. from the NIH (R01CA131797, R01CA140295), NSF (0645080), and UW. S.H.H. thanks Prof. S.Y. Chen and the Nat. Sci. Council of Taiwan for a study abroad fellowship. We are also grateful to UW-NTUF for TEM and SEM, Dr. Y.A. Wang at Oceannanotech for the MNPs, Profs. A. Hoffman and S. Pun for fruitful discussions, and X. Zhang for computer graphics.

Supporting Information Available: Detailed experimental procedure and solubility of MNP and polymer. This material is available free of charge via the Internet at http://pubs.acs.org.

References

(1) (a) Gao, J.; Gu, H.; Xu, B. *Acc. Chem. Res.* **2009**, *42*, 1097–1107. (b) Gao, X. H.; Cui, Y. Y.; Levenson, R. M.; Chung, L. W. K.; Nie, S. M. *Nat. Biotechnol.* **2004**, *22*, 969–976.
(2) Jin, Y. D.; Gao, X. H. *Nat. Nanotechnol.* **2009**, *4*, 571–576.
(3) (a) Gu, H.; Zheng, R.; Zhang, X.; Xu, B. *J. Am. Chem. Soc.* **2004**, *126*, 5664–5665. (b) Gu, H.; Yang, Z.; Gao, J.; Chang, C. K.; Xu, B. *J. Am. Chem. Soc.* **2004**, *127*, 34–35. (c) Teranishi, T.; Inoue, Y.; Nakaya, M.;

Oumi, Y.; Sano, T. *J. Am. Chem. Soc.* **2004**, *126*, 9914–9915. (d) Xu, C.; Wang, B.; Sun, S. *J. Am. Chem. Soc.* **2009**, *131*, 4216–4217. (e) Yu, H.; Chen, M.; Rice, P. M.; Wang, S. X.; White, R. L.; Sun, S. *Nano Lett.* **2005**, *5*, 379–382. (f) Mokari, T.; Rothenberg, E.; Popov, I.; Costi, R.; Banin, U. *Science* **2004**, *304*, 1787–1790.

(4) Behrend, C. J.; Anker, J. N.; McNaughton, B. H.; Brasuel, M.; Philbert, M. A.; Kopelman, R. *J. Phys. Chem. B* **2004**, *108*, 10408–10414.

(5) Sheridon, N. K.; Richley, E. A.; Mikkelsen, J. C.; Tsuda, D.; Crowley, J. M.; Oraha, K. A.; Howard, M. E.; Rodkin, M. A.; Swidler, R.; Sprague, R. *J. Soc. Info. Display* **1999**, *7*, 141–144.

(6) Yamada, K.; Kasai, S.; Nakatani, Y.; Kobayashi, K.; Kohno, H.; Thiaville, A.; Ono, T. *Nat. Mater.* **2007**, *6*, 270–273.

(7) Crossley, S.; Faria, J.; Shen, M.; Resasco, D. E. *Science* **2010**, *327*, 68–72.

(8) (a) Christian, D. A.; Tian, A.; Ellenbroek, W. G.; Levental, I.; Rajagopal, K.; Janmey, P. A.; Liu, A. J.; Baumgart, T.; Discher, D. E. *Nat. Mater.* **2009**, *8*, 843–849. (b) Liu, L.; Ren, M.; Yang, W. *Langmuir* **2009**, *25*, 11048–11053. (c) Yuet, K. P.; Hwang, D. K.; Haghgooie, R.; Doyle, P. S. *Langmuir* **2010**, *26*, 4281–4287. (d) Hong, L.; Jiang, S.; Granick, S. *Langmuir* **2006**, *22*, 9495–9499. (e) Yin, Y.; Lu, Y.; Xia, Y. *J. Am. Chem. Soc.* **2001**, *123*, 771–772. (f) Nie, Z.; Li, W.; Seo, M.; Xu, S.; Kumacheva, E. *J. Am. Chem. Soc.* **2006**, *128*, 9408–9412. (g) Lattuada, M.; Hatton, T. A. *J. Am. Chem. Soc.* **2007**, *129*, 12878–12889. (h) Shah, R. K.; Kim, J.-W.; Weitz, D. A. *Adv. Mater.* **2009**, *21*, 1949–1953. (i) Roh, K. H.; Martin, D. C.; Lahann, J. *Nat. Mater.* **2005**, *4*, 759–763.

(9) Kietzke, T.; Neher, D.; Kumke, M.; Ghazy, O.; Ziener, U.; Landfester, K. *Small* **2007**, *3*, 1041–1048.

(10) Isojima, T.; Suh, S. K.; Vander Sande, J. B.; Hatton, T. A. *Langmuir* **2009**, *25*, 8292–8298.

(11) Saito, N.; Kagari, Y.; Okubo, M. *Langmuir* **2006**, *22*, 9397–9402.

(12) Kim, D.-H.; Rozhkova, E. A.; Ulasov, I. V.; Bader, S. D.; Rajh, T.; Lesniak, M. S.; Novosad, V. *Nat. Mater.* **2009**, *9*, 165–171.

(13) Kim, H.; Ge, J.; Kim, J.; Choi, S.-e.; Lee, H.; Lee, H.; Park, W.; Yin, Y.; Kwon, S. *Nat. Photon.* **2009**, *3*, 534–540.

(14) Lee, J. H.; Huh, Y. M.; Jun, Y. W.; Seo, J. W.; Jang, J. T.; Song, H. T.; Kim, S.; Cho, E. J.; Yoon, H. G.; Suh, J. S.; Cheon, J. *Nat. Med.* **2007**, *13*, 95–99.

JA102489Q